

# Models of Planets and Brown Dwarfs in Mira Winds

Curtis Struck<sup>1</sup>, Babak E. Cahanim, and Lee Anne Willson<sup>2</sup>

*Department of Physics and Astronomy Department, Iowa State University, Ames, IA 50011*

## ABSTRACT

We present numerical hydrodynamical models of the effects of planets or brown dwarfs orbiting within the extended atmosphere and wind formation zone of Mira variables. We find time-dependent wake dynamics and episodic accretion phenomena which may give rise to observable optical events and affect SiO maser emission.

*Subject headings:* stars: planetary systems - stars: winds, outflows - stars: variables - stars: AGB and Post-AGB - accretion, accretion disks - masers

## 1. Introduction

When stars like the Sun evolve to become AGB stars, their outer envelopes swell to sizes of order an astronomical unit (au). During the AGB phase the star becomes unstable to large amplitude radial pulsations, and becomes a Mira or semi-regular variable (e.g., Hansen & Kawaler (1994)). These pulsations drive strong shock waves down the steep pressure gradient outside the photosphere, producing an extended atmosphere, and a dense, warm stellar wind (Bowen (1988), also see Willson (2000)). In the most luminous stars the wind driving is also enhanced by radiation pressure on dust grains that form a few stellar radii from the photosphere (e.g., Bowen (1988), Gail & Sedlmayr (1999), Willson (2000)). During the Mira phase it is likely that the winds are primarily radial since the massive, extended stellar atmosphere cannot have significant rotation, and at this stage it is unlikely that a globally ordered magnetic field strongly affects the dynamics of the wind (see Soker & Zoabi (2002)).

In recent years, about 80 extrasolar planetary systems have been discovered (Butler, et al. 2001). Generally, these systems have a single gas giant planet, with a mass of up to

---

<sup>1</sup>Dept. of Physics and Astronomy, 12 Physics Bldg., Iowa State Univ., Ames, IA 50011, curt@iastate.edu

<sup>2</sup>lwillson@iastate.edu

$\simeq 15$  Jupiter masses ( $M_J$ ), and an orbital semi-major axis of commonly less than 1.0  $au$ , but ranging up to  $\simeq 4.0$   $au$  (e.g., Hatzes, et al. (2000), Fischer, et al. (2002)). Increasing numbers of brown dwarf stars have also been discovered recently. Most of these brown dwarfs are not companions of main sequence Mira progenitors (but see Fischer, et al. (2002), Liu, et al. (2002)). The more massive “planets” are in fact low mass brown dwarfs, and they make up a significant fraction of the extrasolar ‘planetary’ systems.

The interaction between Mira winds and giant planets or low-mass brown dwarfs with small orbital radii is an intriguing topic. This is especially true in light of the distortion observed in the outflow in the *o Ceti* system, apparently as a result of its (more distant) white dwarf companion (Karovska, et al. 1997). The class of symbiotic systems containing a Mira and a dwarf companion are also similar. Jura and collaborators (Jura & Kahane 1999, and refs. therein) have studied other interesting giant star binary systems, with molecular reservoirs and dust rings. We cannot hope to observe close planet systems in the same detail as these related systems. As we will describe below, observational signatures are likely to be indirect (see Willson & Struck (2001)).

Because planetary orbital periods (e.g., 3-30 yr.) are roughly similar to wind crossing times over radial scales of about 1.0  $au$  (.5 - 3.0 yr.), massive planets will create substantial wakes, and perturb the local wind flow. Within about 5  $au$ , the motion of the extended stellar atmosphere is still primarily oscillatory. The oscillating atmospheric gas elements and the propagating shocks interact with the planetary bow shock and wake, so the resulting flow is complex and very time-dependent. The planet accretes gas out of the stellar wind, but the amount of mass accreted over the AGB lifetime is very small compared to the planet’s mass (Willson & Struck 2001, and below). Gas drag on Jovian planets and brown dwarfs will also be small, unless they orbit very close to the star, i.e., within the atmosphere (Willson & Bowen 2002).

Nonetheless, the accretion may release enough energy, in a suitable form, to give rise to observable events. E.g., Willson & Struck (2001) argue that episodic optical flashes like those reported in the literature (e.g., de Laverny, et al. (1998), Schaefer (1991), Stencel, et al. (2001)) may be produced. Moutou, et al. (2001) have also suggested that wake-like cometary ‘exospheres’ of giant planets, orbiting near their parent stars, might be observable. The planetary perturbation may affect other still observables, like the SiO maser emission that arises from the same region (Struck-Marcell 1988). To further understand both the observational signatures and the basic dynamics of the interaction, we have undertaken a program of hydrodynamic modeling of such systems, and present the first results below.

Ultimately, the observational signatures of planets or brown dwarfs in Mira winds could provide a new means of discovering such companions, and of learning more about their fates

in the late stages of stellar evolution.

## 2. Models

The model results presented below were produced with a smoothed particle hydrodynamics (SPH) code, in which hydrodynamic forces are computed with a spline kernal on a grid with a fixed, uniform cell size. A standard artificial viscosity formulation is used to model shocks. The code is described in detail in Struck (1997).

Both stellar and planet gravities were approximated as softened point masses, though with small softening lengths. The SPH smoothing length was set to 0.1 length units, where the unit of length was chosen to be 1.0 au.

Initially 38500 gas particles were placed over a quarter annulus in the orbital plane of the planet, and on a circular coordinate grid with constant radial intervals and a constant number of particles on each azimuthal arc. This distribution yields a  $1/r^2$  density profile (in three dimensions), similar to that observed. The particles were then given slight random offset from the initial grid and a small random velocity in the plane, to smooth the distribution. Initial radial and azimuthal velocities were zero except for this random part.

The models were run with a three dimensional code, but the model is essentially two dimensional, since the particles were initialized in a ( $z = 0$ ) plane, with zero vertical velocity. No vertical motions developed throughout the runs.

An isothermal equation of state was used with the particle internal energy set to a value corresponding to  $T \simeq 1700K$ . In the absence of dust the detailed Mira atmosphere models of Bowen (1988) show that there are large temperature variations. However, if there is even a small amount of dust, then the gas is roughly isothermal over the radial range of the present model at about the adopted temperature.

We neglect radiation pressure on grains, assuming that the size and abundance of grains is small. Bowen's models suggest that grains form just inside the radial range considered here, and that radiation pressure exceeds the outward push of pulsational shocks in the outer part of this region in solar metallicity stars. However, the application of a nearly zero pressure upper boundary condition suppresses the oscillatory motion and gives rise to a wind at the largest radii in our model, with an overall flow much like Bowen's models.

For the boundary conditions in these preliminary models we have employed some simple approximations. First, the sides (near the x and y axes) are reflective boundaries, which have little effect since the motion is primarily radial. Secondly, the outer bound is initially

at a radius of 4.0 au, with the planet on a circular orbit of radius 3.5 au, and is moved steadily outward at a velocity of  $V_{shock} = 2.0$  units (or about 14.  $km/s$ ) for the duration of the run. Because pulsational shocks give particles near the outer bound outward impulses on timescales shorter than the fractional free-fall time needed to return to their initial positions, gas particles move outward. The outer bound is moved outward to prevent excessive interaction between it and the particles.

Thirdly, the inner boundary moves outward and inward on a cycloidal trajectory from an initial radius of 2.0 *au*. The period of this motion is close to that of a ballistic particle at that radius, so particles in that region track it quite closely.

The final boundary condition is applied on a circle of radius 0.08*au* around the planet. Any particles moving within this circle are assumed to be captured by the planet, and thus, are immediately transferred to the planet center, and given the same velocity as the planet. The radius of this circle equals about 170 Jupiter radii, but since it is slightly less than the adopted SPH smoothing length, it is at the resolution limit of the simulation. Although we will continue to refer to it as a planet, its mass was chosen to be  $30M_J$ , which is in the brown dwarf range. With this relatively large mass the gravity of the planet is large enough to show all the essential hydrodynamics on a grid of modest resolution which contains a significant part of the orbit. We see the same hydrodynamic effects on a smaller scale with less massive planets, but those calculations require a smaller scale grid, or many more particles.

### 3. Model Results

Figure 1 shows six snapshots from a representative model. Over the course of this run the planet enters the grid from below and moves around the quadrant, while several pulsational shocks are generated at the base and move through the grid. At the beginning of the run (not shown) the planet enters the grid and begins to form a bow shock and wake, while a shock is generated at the inner boundary. This and subsequent pulsational shocks move through the grid and fairly quickly set up a pattern of radial motions much like those in Bowen’s models (Bowen 1988). That is, particle motions are primarily oscillatory in the inner part of the grid and primarily outflowing in the outer part (see Figure 2). Weak reflection shocks from the outer boundary have a small effect on the radial motions of the particles.

As an outward propagating shock sweeps over the planet the wake is pushed into a more outward pointing configuration. As material falls back in the rarefaction behind the shock, the wake reforms in an azimuthal or slightly inward direction. At most times the wake has

a visible extent of at least 2 *au*. Figure 1 also shows that downstream shock fronts are disturbed.

The insets in Figure 1, show how the planet accretes gas out of the wake. Wake accretion generally exceeds direct accretion. In most cases the accretion occurs via a single dominant stream. This stream has nonzero angular momentum relative to the planet, and so it spirals into the planet, rather than falling radially.

The direction and amount of particle angular momentum relative to the planet depends on the particle’s radial velocity, which depends on the phase of the local pulsation cycle. In particular, as shown in the Figure 1 insets, infalling gas spirals around the planet alternately in the clockwise and counter-clockwise directions.

Figure 3 shows the cumulative number of particles accreted as a function of time. Initially, while the wake is developing, the accretion is quite steady. Later the accretion becomes episodic, reflecting the time-dependence of the input stream from the wake. This stream develops first in one sense, then as a result of the shocks and radial flow reversals, the stream is first cut off, then re-established in the opposite sense.

This alternating flow is reminiscent of the flip-flop instability discussed in the literature on Bondi-Hoyle-Lyttleton accretion by compact companions in OB star winds (see Benensohn, et al. (1997), Ruffert (1999) and Foglizzo & Ruffert (1999) and references therein). The idea of reversing accretion disks has also been considered in this context by Murray, De Kool, & Li (1999). However, in these cases, the flip-flop instability is self-excited, and operates on an acoustic timescale. In the present case, the ‘flip-flop’ is driven on a pulsational timescale. It appears that the peak to mean accretion rate ratio in the present case is higher than in self-excited cases.

Figure 2, and other graphs not shown here, show that the planet accelerates a significant amount of material in the azimuthal direction. Indeed, at the end of the run, wake particles can still be detected at all azimuths by their azimuthal velocities. In the future we plan to study this effect over a full orbit.

#### 4. Observational Consequences

When the accretion stream flow changes direction, any accretion disk that has formed around the planet from earlier streaming (not resolved in our simulations), is likely to be severely disrupted. Most of the accreted material probably falls onto the planet, dissipating its infall energy.

We can estimate the rate of energy dissipation from the simulation. Hydrodynamic variables like the density are dimensionless in the code. We scale the initial density profile by assuming that it is essentially the same as the time-averaged density profile in a dust-free, model of Bowen (1988). In both cases the density profile has approximately a  $1/r^2$  form, and in the representative Bowen model with  $\dot{M} = 1.5 \times 10^{-7 \pm 2} M_{\odot} \text{yr}^{-1}$ , the density is about  $2.0 \times 10^{-15}$  at 4.0 a.u. We estimate the total simulation volume as the initial area containing the particles times a thickness of twice the SPH softening length (i.e., 0.2 au). Then with the given number of particles and the density profile the mass per particle is  $\simeq 2.5 \times 10^{21} g$ . We estimate the energy released in an accretion burst as,

$$\begin{aligned} \Delta E &= \frac{1}{2} m_p N_b v_{ff}^2 \simeq 6.8 \times 10^{37} \text{ ergs} \\ &\times \left( \frac{m_p}{2.5 \times 10^{21} g} \right) \left( \frac{N_b}{50} \right) \left( \frac{v_{ff}^2}{330. \text{ km/s}} \right), \end{aligned} \quad (1)$$

where  $m_p$  is the particle mass,  $N_b$  is the number of particles accreted in the event, and  $v_{ff}$  is the free-fall velocity at the planet's surface. The scaled value of  $v_{ff}$  in the last equality assumes a planet mass of  $30M_J$ , and radius of  $R_J \simeq 7.0 \times 10^9 \text{ cm}$ . The value of  $N_b$  is that derived from the model, with no correction for the cross section of the bow shock in three dimensions, since the vertical extent assumed in making the particle mass normalization is about the same as the bow shock radius.

The luminosity of the accretion burst is about,

$$\begin{aligned} L &= \frac{\Delta E}{\tau_{ff}} \simeq 6.5 \times 10^{33} \text{ ergs s}^{-1} \\ &\times \left( \frac{3.0 \text{ hrs.}}{\tau_{ff}} \right) \left( \frac{M}{30. M_J} \right)^{3/2}, \end{aligned} \quad (2)$$

where the free-fall time of 3.0 hours is evaluated at ten planetary radii. Such short timescales cannot be resolved by the numerical model. However, we have measured the angular momentum of gas elements just before they are accreted. The circular orbital radii corresponding to the measured angular momenta are of the order of 3 – 10 planetary radii, suggesting that this is the correct scale for an accretion disk formed from this material.

The luminosity estimate above is about  $1.7 L_{\odot}$ , yet there are several reasons to believe that it could be higher. In models with dust, or larger amplitude pulsations, values of mass loss and wind density can be increased by two orders of magnitude. Moreover, with a magnetotail to interfere with the downstream motion of particles in the pulsational wave, the planet could acquire more. Thus, it is very possible that the burst luminosity could

substantially exceed a solar luminosity in some cases. Any luminosity above  $0.01L_{\odot}$  is potentially detectable in a Mira near minimum light.

Given the large free-fall velocity it is likely that much of the energy is initially radiated in the UV and X-ray bands. A sphere of radius  $\simeq 10R_J$  around the planet (or a hemisphere) will be ionized. Much of this energy will be reprocessed and escape in the form of optical continuum and emission line radiation. Thus, the simulation provides some support for the conjecture of Willson & Struck (2001) that short timescale optical flashes from Miras could be the result of this process.

In reality, the accretion process must be very complex. For example, the coupling of the partially ionized gas to the planetary magnetic field could induce a variety of additional effects. These might include sporadic magneto-centrifugal jets, or energetic reconnection events, but the relation of such processes to observables would require more detailed models.

The complex dynamics induced by large planets almost certainly affect another phenomenon of this region in Mira winds, the SiO maser emission. Some aspects of this interaction were described by Struck-Marcell (1988). For recent observational results see Boboltz & Marvel (2000), Diamond, et al. (2001), and references therein. Here we note that the nonlinear perturbations in the planetary wake could have a significant effect on the pumping of SiO molecules. The models show that density perturbations persist and extend for a long distance behind the planet, perhaps over most of the orbital circumference. The density amplitudes are also likely to be underestimated since the isothermal models do not allow for the development of thermal instabilities (e.g., mediated via SiO itself, see Muchmore, Nuth, & Stencel (1987)). Maser emission may be enhanced near the planet in the accretion process, or indirectly, from radiative pumping following accretion bursts. As noted by Struck-Marcell (1988) the proximity of the planetary magnetosphere and magnetotail, help account for high SiO maser polarizations.

Because of the nonlinear amplification in maser emission, it may provide a particularly sensitive probe of Mira planets and close stellar companions. Monitoring of optical flashes, on the other hand, provides a relatively simple means of searching many systems for possible companions, especially brown dwarf companions. The discovery and study of such companions would open a new window for the study of the properties and population systematics of brown dwarfs and giant planets.

We are grateful to G. H. Bowen for numerous helpful conversations and unpublished model results. We are also grateful to Agnes Bishoff for helpful conversations, and to the referee for pointing out the flip-flop literature.

## REFERENCES

- Benenohn, J. S., Lamb, D. Q., & Taam, R. E. 1997, *ApJ*, 478, 723
- Boboltz, D. A., & Marvel, K. B. 2000, *ApJ*, 545, 149
- Bowen, G. H. 1988, *ApJ*, 329, 299
- Butler, R. P., Marcy, G. W., Fischer, D. A., Vogt, S. S., Tinney, C. G., Jones, H.R.A., Penny, A.J., & Apps, K., 2000., to appear in, *Planetary Systems in the Universe: Observations, Formation and Evolution*, ASP Conf. Series, 2001, eds. A.Penny, P.Artymowicz, A.-M. Lagrange, and S. Russell, San Francisco: ASP (also see: <http://exoplanets.org/>)
- de Laverny, P., Mennessier, M. O., Mignard, F., & Mattei, J. A. 1998, *A&A*, 330, 169
- Diamond, P. J., et al. in *Galaxies and Their Constituents at the Highest Angular Resolution*, I.A.U. Sym. 205, eds. R. T. Schilizzi, S. Vogel, F. Paresce, & M. Elvis, San Francisco: ASP, p. 14
- Fischer, D. A., Marcy, G. W., Butler, R. P., Laughlin, G., & Vogt, S. S. 2002, *ApJ*, 564, 1028
- Gail, H.-P., & Sedlmayr, E. 1999, *A&A*, 347, 594
- Foglizzo, T., & Ruffert, M. 1999, *A&A*, 347, 901
- Hansen, C. J., & Kawaler, S. D. 1994, *Stellar Interiors: Physical Principles, Structure and Evolution*, New York: Springer
- Hatzes, A. P., et al. 2000, *ApJ*, 544, 145
- Jura, M., & Kahane, C. 1999, *ApJ*, 521, 302
- Karovska, M., Hack, W., Raymond, J., & Guinan, E. 1997, *ApJ*, 482, 175
- Liu, M. C., Fischer, D., Graham, J. R., Lloyd, J. P., Marcy, G. W., & Butler, R. P. 2002, *ApJ*, in press (astro-ph 0112407)
- Moutou, C., Coustenis, A., Schneider, J., St. Giles, R., Mayor, M., Queloz, D., & Kaufer, A. 2001, *A&A*, 371, 260
- Muchmore, D. O., Nuth, J. A., III, & Stencel, R. E. 1987, *ApJ*, 315, 141
- Murray, J. R., De Kool, M., & Li, J. 1999, *ApJ*, 515, 738

- Ruffert, M. 1999, A&A, 346, 861
- Schaefer, B. 1991, ApJ, 366, 39
- Soker, N. & Zoabi, E. 2002, MNRAS, 329, 204
- Stencel, R. E., Phillips, A., Jurgenson, C., & Ostrowski-Fukuda, T. 2001, BAAS, 199, 9219
- Struck, C. 1997, ApJS, 113, 269
- Struck-Marcell, C. 1988, ApJ, 330, 986
- Willson, L. A. 2000, ARA&A, 38, 573
- Willson, L. A., & Bowen, G. H. 2002, in prep.
- Willson, L. A., & Struck, C. 2001, JAAVSO, 30, 23

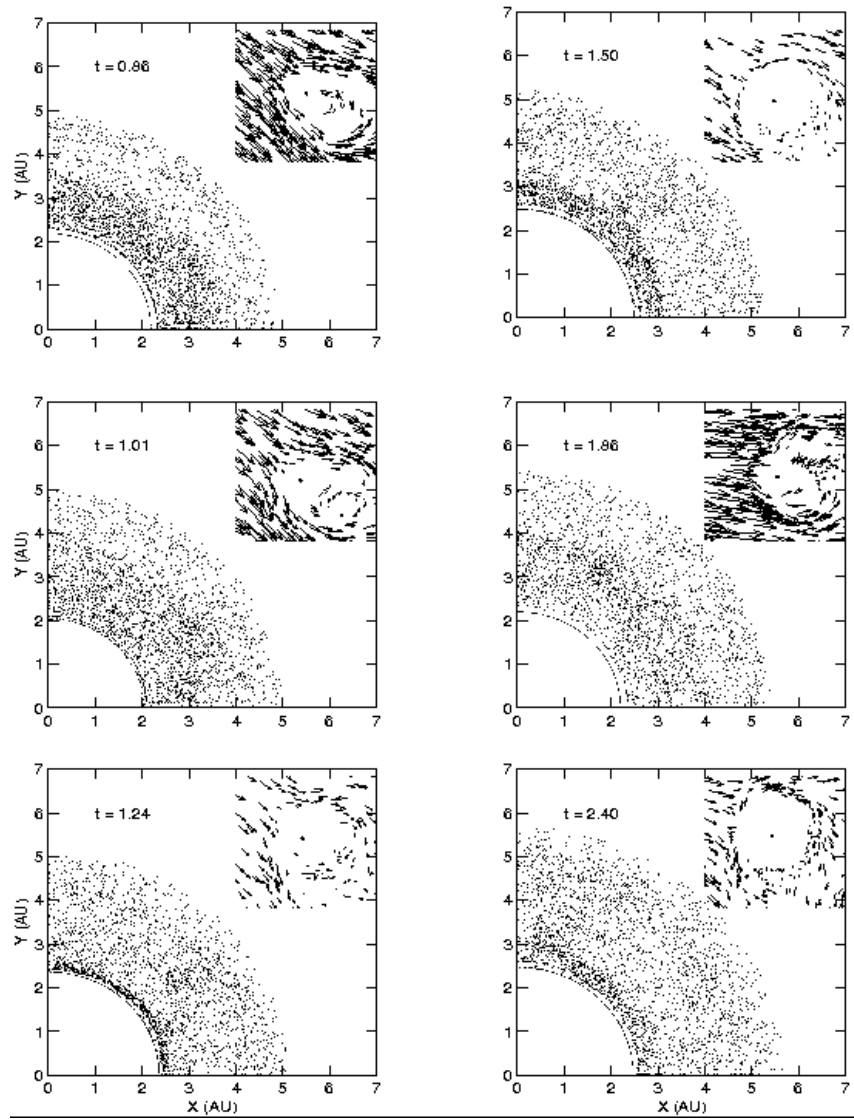


Fig. 1.— Particle positions at 6 representative times. Several pulsational shocks are shown, and the motion of the planet and the evacuated region around it is also clear. The continually changing structure of the planetary wake is evident. The accretion stream into the evacuated region also has a different appearance in each snapshot. This is emphasized in the insets, which show selected particles in a small region around the planet, with velocity vectors of length proportional to the particle’s speed. Note the strong counterclockwise inflow at  $t = 0.86$  and  $1.86$  units, when the shock has just passed the planet, and also the clockwise inflow at  $t = 1.24$  when the planet is in the middle of the post-shock rarefaction.

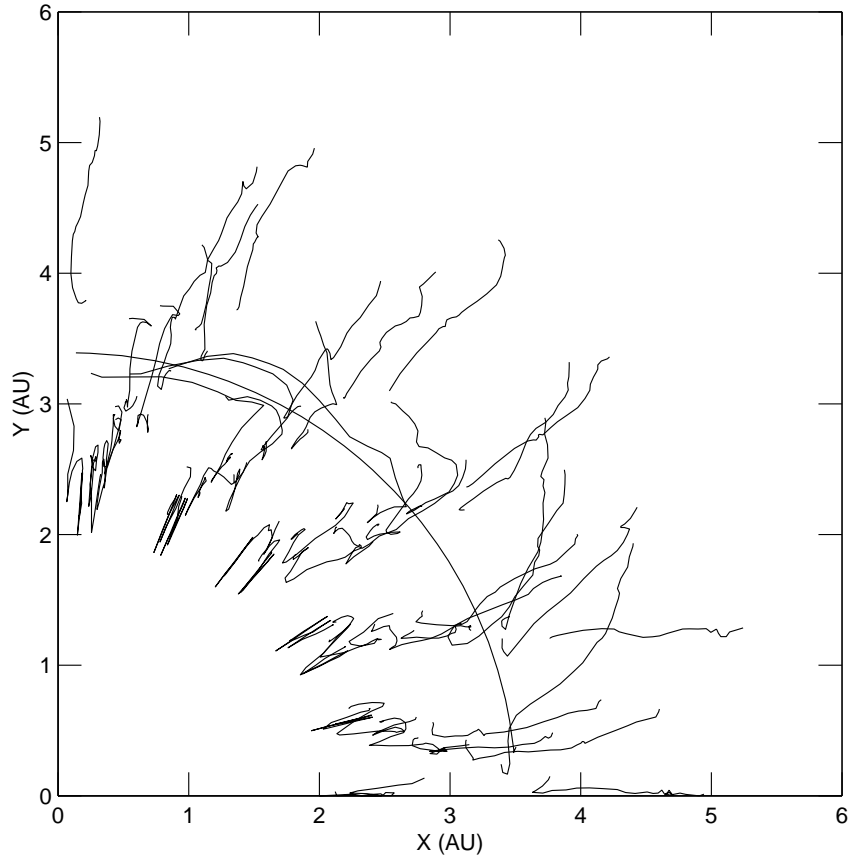


Fig. 2.— The  $xy$  trajectories of a sample of a few tens of particles. Note the oscillatory motion at smaller radii and the generally outward motion at large radii. This figure highlights the effects of the planet's gravity on particles, which would have only radial motions in the absence of the planet. The trajectory of the planet is marked by a particle captured at early times.

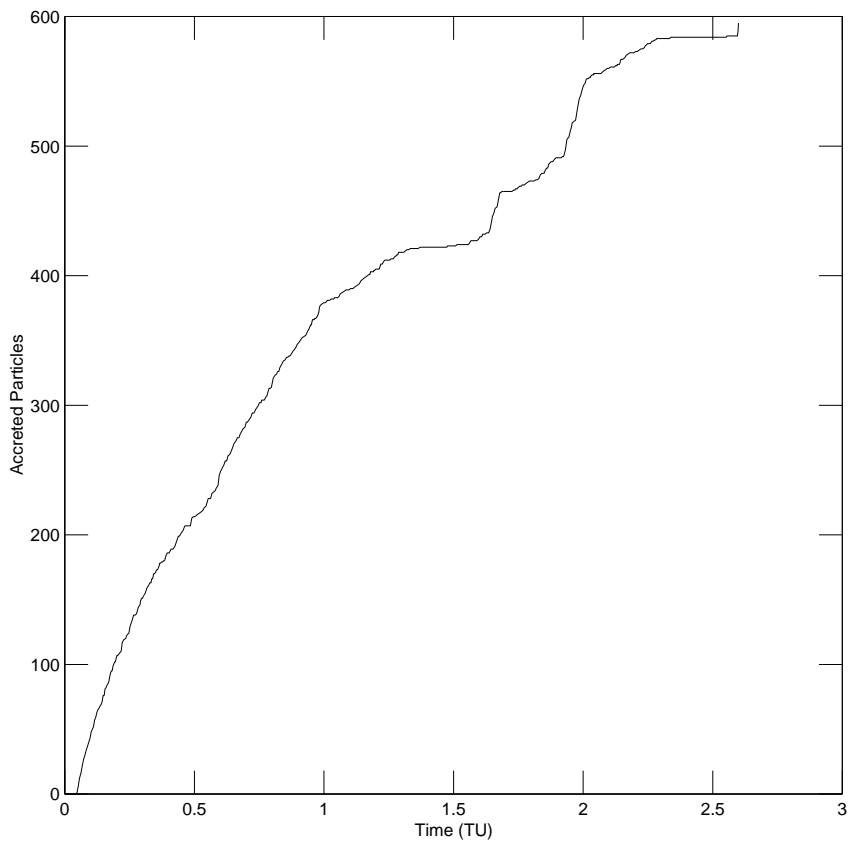


Fig. 3.— Cumulative number of particles accreted by the planet as a function of time. Note the development of episodic accretion.